

Original Paper

# Intermittent Hypoxia and Its Impact on Nrf2/HIF-1 $\alpha$ Expression and ABC Transporters: An *in Vitro* Human Blood-Brain Barrier Model Study

Cindy Zolotoff<sup>a,b</sup> Anne-Cloé Voirin<sup>a,b</sup> Clémentine Puech<sup>b</sup> Frédéric Roche<sup>b,c</sup>  
Nathalie Perek<sup>a</sup>

<sup>a</sup>INSERM, U1059, Sainbiose, Dysfonction Vasculaire et Hémostase, Université de Lyon, Université Jean Monnet, Saint-Etienne, France, <sup>b</sup>EA 4607 Système Nerveux Autonome – Epidémiologie Physiologie Ingénierie Santé, Université de Lyon, Université Jean Monnet, Saint-Priest-en-Jarez, France, <sup>c</sup>Service de Physiologie Clinique et de l'Exercice, Centre VISAS, CHU, Saint Etienne, France

## Key Words

Intermittent hypoxia • Oxidative stress • Blood brain-barrier model • ABC transporters • Tight junction proteins

## Abstract

**Background/Aims:** Obstructive sleep apnea (OSA) is characterized by repeated episodes of complete or partial obstruction of the upper airways, leading to chronic intermittent hypoxia (IH). OSA patients are considered at high cerebrovascular risk and may also present cognitive impairment. One hypothesis explored is that disturbances may be linked to blood-brain barrier (BBB) dysfunction. The BBB is a protective barrier separating the brain from blood flow. The BBB limits the paracellular pathway through tight and adherens junctions, and the transcellular passage by efflux pumps (ABC transporters). The aims of this study were to evaluate the impact of IH and sustained hypoxia (SH) on a validated *in vitro* BBB model and to investigate the factors expressed under both conditions. **Methods:** Exposure of endothelial cells (HBEC-5i) in our *in vitro* model of BBB to hypoxia was performed using IH cycles: 1% O<sub>2</sub>-35 min/18% O<sub>2</sub>-25 min for 6 cycles or 6 h of SH at 1% O<sub>2</sub>. After exposure, we studied the cytotoxicity and the level of ROS in our cells. We measured the apparent BBB permeability using sodium fluorescein, FITC-dextran and TEER measurement. Whole cell ELISAs were performed to evaluate the expression of tight junctions, ABC transporters, HIF-1 $\alpha$  and Nrf2. The functionality of ABC transporters was evaluated with accumulation studies. Immunofluorescence assays were also conducted to illustrate the whole cell ELISAs. **Results:** Our study showed that 6 h of IH or SH induced a BBB disruption marked by a significant decrease in junction protein expressions (claudin-5, VE-cadherin, ZO-1) and an increase in permeability. We also observed an upregulation in

N. Perek and F. Roche contributed equally to this work.

P-gp protein expression and functionality and a downregulation in BCRP. Hypoxia induced production of ROS, Nrf2 and HIF-1 $\alpha$ . They were expressed in both sustained and intermittent conditions, but the expression and the activity of P-gp and BCRP were different. **Conclusion:** Understanding these mechanisms seems essential in order to propose new therapeutic strategies for patients with OSA.

© 2020 The Author(s). Published by  
Cell Physiol Biochem Press GmbH&Co. KG

## Introduction

Obstructive sleep apnea (OSA) is a serious sleep disorder affecting approximately 5% of the adult population over 45 years old and more than 10% after 65. OSA is characterized by repeated episodes of complete or partial obstruction of the upper airways during sleep, resulting in chronic cyclical intermittent hypoxia (IH) [1]. IH plays a crucial role in the increase of cardiovascular and cerebrovascular risks [2]. Increasing data support a time relationship between OSA and cognitive impairment [3], but a causal link has yet to be established. A hypothesis has been raised [4] in which IH acts as a biostressor that could disrupt the blood-brain barrier (BBB) via molecular responses. Adaptive responses at the BBB level may occur specifically through regulation of BBB transporters, like the ATP binding cassette (ABC) transporter family when altering BBB microvessel permeability. These changes in BBB transporters may have long-term consequences that alter the brain's microenvironment, leading in the long-term to cognitive impairment [4].

The BBB is a protective barrier separating the brain from blood flow and is composed primarily of endothelial cells closely related to astrocytes, pericytes and neurons, which together form the neurovascular unit [5]. The BBB has tight [6] and adherens junctions [7] which allow it to control the exchanges between the brain and blood flow and to limit permeability.

Furthermore, the transmembrane proteins that make up the tight junctions (TJ) (zonula occludens (ZO)-1, claudin-5, etc.) and adherens junctions (e.g., vascular endothelial (VE)-cadherin), limit the paracellular transfer of molecules [8] and strengthen interactions between endothelial cells. Brain microvessel endothelial cells also express transporters that will allow blood-brain regulation and adaptation such as ATP ABC transporters, and more precisely breast cancer resistance protein (BCRP) and/or P-glycoprotein (P-gp) [9]. These two latter transporters are the most expressed and involved at the human BBB level. Moreover, P-gp may efflux xenobiotic components or glutamate [4] and BCRP is involved in the efflux in the blood flow of uric acid [10]. All those microstructural cell elements are essential to ensure the functional integrity of the BBB. Thus, under hypoxic conditions, many factors are secreted and induce a modification in the expression of junction proteins or in the activity of ABC transporters. IH or sustained hypoxia (SH) produces reactive oxygen species (ROS) [11] that lead to oxidative stress [12, 13] and contribute to inflammatory cascades [14]. Indeed, the formation and accumulation of ROS in hypoxic cells is a hallmark of hypoxia involved in BBB dysfunction [15]. In association with the production of ROS, several factors are activated or stabilized. Effectively, hypoxia-inducible factor 1 (HIF-1), and more specifically HIF-1 $\alpha$ , is stabilized [16] and stimulates the transcription of genes involved in various biological processes such as angiogenesis, cell proliferation, inflammation or cancer [17, 18]. Nuclear factor erythroid 2-related factor 2 (Nrf2) expression is also modulated in response to hypoxia [19]. Nrf2 controls the expression of antioxidant defence genes under hypoxic conditions, allowing cells to regulate the oxidative stress mediated ROS species. Nrf2 regulates the expression of these genes by binding to antioxidant response elements in their promoter regions, which reduce the levels of damaging ROS in the cell [20]. Those transcription factors are known to modify the expression and activity of ABC transporters, such as HIF-1 $\alpha$  which induces an increase in P-gp expression in hypoxia colon carcinoma cells [21] and a decrease in BCRP expression [22] in choriocarcinoma cells also under hypoxia. To determine how IH causes adaptative metabolic response at the BBB level, implying Nrf2,

HIF-1 $\alpha$  and ABC transporter expressions, we proposed to use a human *in vitro* BBB model developed in our laboratory [23] and setting up a model of intermittent hypoxic exposure.

Currently, there are few *in vitro* models to study the effects of IH encountered in OSA. Indeed, there are no standardized protocols. Some studies carried out “short” cycles (3 min of normoxia followed by 15 s of hypoxia) [24, 25], others were “longer” (25 min of hypoxia followed by 35 min of normoxia [26, 27] or 1 h of hypoxia followed by 30 min of normoxia [28]). Each model has advantages and disadvantages. The severity of hypoxia also seems to vary greatly between the different models [29]. We chose 1% oxygen in the environment of the cell that represents the pathological percentage of oxygen exposure observed in the *in vivo* brain. We therefore decided to develop our own model with alternating 35 min cycles of hypoxia at 1% O<sub>2</sub> followed by cycles of reoxygenation with 18% O<sub>2</sub> for 25 min during 6 cycles on our model of BBB. The 6-h duration is important and representative of one short night similar to the pathological conditions found in OSA. For the human *in vitro* BBB model, we used HBEC-5i human brain endothelial cells and human astrocyte (HA) conditioned medium [23]. We first looked at the effects of this IH on a human BBB model: transendothelial electrical resistance (TEER) and apparent permeability (P<sub>app</sub>) with the expression of VE-cadherin, claudin-5 and ZO-1 junction proteins. Then ABC transporter (P-gp, BCRP) expression and functionality were evaluated with accumulation studies and fluorescent selective substrates and inhibitor combinations. We also evaluated the level of intracellular ROS and the expression of two transcriptional factors expressed under hypoxic conditions, such as Nrf2 and HIF-1 $\alpha$ .

The purpose of the study was to 1) compare the effects of SH and IH, 2) quantify protein expressions of junctions and ABC transporters, 3) characterize the effects of IH on the activity of ABC transporters, and 4) identify the expression of Nrf2 and HIF-1 $\alpha$  under IH and SH.

## Materials and Methods

### *Chemicals and reagents*

Cell culture inserts for 24-well plates (high density pore, 0.4- $\mu$ m pore diameter size, translucent polyterephthalate ethylene (PET) membrane, culture flasks and companion plates were purchased from Dominique Dutscher (Strasbourg, France). Imaging plates FC, 96 wells, TC-surface were purchased from MoBiTec (Goettingen, Germany).

Rabbit polyclonal to VE-cadherin (VE-cadherin-ab33168) for ELISA and immunofluorescence (IF) were purchased from Abcam (Cambridge, United Kingdom). Rabbit polyclonal anti-ZO-1 (ZO-1-ab59720) for IF was purchased from Abcam (Cambridge, United Kingdom). Secondary antibodies for IF: goat anti-rabbit antibodies (A-21127 Alexa Fluor 488), DAPI for microscopy and superFrost™ were obtained from Thermo Fisher Scientific (Waltham, USA). Mouse monoclonal IgG anti-ABCG2 (sc-18841), mouse monoclonal anti-rabbit IgG to P-gp (sc-390883), mouse monoclonal anti-claudin-5 (sc-374221) and secondary antibody for cell ELISA mIgG BP-HRP (sc-516102) were purchased from Santa Cruz Biotechnology (Dallas, Texas, USA). Rabbit ZO-1 polyclonal antibody for ELISA (40-2200), Dulbecco's Modified Eagle Medium/Nutrient Mixture F-12 (11330057), rhodamine-123, secondary antibodies for IF: goat anti-rabbit antibodies (A-11034 Alexa Fluor™ 488), DAPI for microscopy, superFrost microscope slide and Coomassie Plus™ protein assay were obtained from Thermo Fisher Scientific (Waltham, USA). Vectashield Antifade mounting medium (H-1000) was purchased from Eurobio Scientific.

OxiSelect™ Intracellular ROS Assay Kit (green fluorescence, STA-342) and HIF-1 $\alpha$  Cell Based ELISA Kit (CBA-281) were purchased from Cell Biolabs (San Diego, USA). NFE2L2 ELISA Kit (human) (OKCD02754) was purchased from Aviva Systems Biology (San Diego, USA).

Astrocyte medium (AM), astrocyte growth supplement (AGS), fetal bovine serum (FBS) and penicillin-streptomycin solution for astrocytes were purchased from CliniSciences (Nanterre, France). Amphotericin B (30-003-CF) and Trypsin 2.21 mM EDTA were purchased from Corning (Manassas, USA). Penicillin-streptomycin (100X) was purchased from PanReac Applichem (Darmstadt, Germany).

All other reagents were purchased from Sigma-Aldrich (St Quentin Fallavier, France).

### *In vitro BBB model*

The BBB model was composed of HBEC-5i endothelial cells (from ATCC-Manassas, VA, USA) and a HA cell line (ScienCell Research Laboratories, Carlsbad, CA, USA) cultured in PET transwells with 0.4- $\mu$ m pores and in plates [23].

Initially, HBEC-5i were cultured in DMEM/F12 HAM, supplemented with 10% FBS, 40  $\mu$ g/mL endothelial cell growth supplement (ECGS) and 1% antibiotic antimycotic solution. HAs were grown in AM containing 2% FBS, 1% AGS and 1% penicillin-streptomycin solution according to manufacturer's instructions. Afterwards, HA were in the same medium as HBEC-5i. In our model, HBEC-5i endothelial cells were in contact with astrocytic conditioned medium. In fact, in addition to playing a role in the induction and long-term maintenance of barriers, astrocytes can release chemical factors that modulate endothelial permeability [30]. The conditioned medium corresponds then to a medium that has remained in contact with the astrocytes for 48 h. For each condition, the medium was renewed every 2 d. HBEC-5i with HA conditioned medium reached an optimal steady state plateau at day 14 which was maintained for 5 d [23]. Cells were cultured at 37°C with 5% CO<sub>2</sub>.

### *Experimental hypoxia and IH protocols*

For this protocol we used a hypoxic workstation: Baker Ruskinn, Invivo<sub>2</sub> 300 and the ICO<sub>2</sub>N<sub>2</sub>IC Advanced Gas Mixing System (Maine, USA). This hypoxia chamber maintained and controlled temperature, oxygen, humidity and carbon dioxide. The ICO<sub>2</sub>N<sub>2</sub>IC provided accurate control over O<sub>2</sub> (0.1%-20.9%) and CO<sub>2</sub> (0.1%-30%). In our model, two incubation conditions were performed: SH or IH. Under SH, cells were incubated for a continued period of 6 h at 1% O<sub>2</sub> and 5% CO<sub>2</sub>. Under IH, cells were exposed to repeated hypoxia (35 min, 1% O<sub>2</sub>)/reoxygenation (25 min, 18% O<sub>2</sub>) for 6 cycles. We decided to use the hypoxia chamber at 1% O<sub>2</sub> since in the brain under physiological conditions, the oxygen level is close to 5%. Thus, we used the lowest level of oxygen possible in which we had no cytotoxic effects on the cells but where a response was observed.

For each condition, DMEM/F12 was conditioned the day before at 1% O<sub>2</sub> in this hypoxic chamber. In order to ensure that the oxygen balance was achieved, we used an oximeter (Multi 3510 IDS, FDO 925, WTW, Germany) to control the percentage of dissolved oxygen within the medium. The conditioned medium of HA was also conditioned according to the two conditions of the model. Control normoxic cells were maintained in normal atmospheric gas pressure.

### *Cytotoxicity assays*

MTT assay was employed to measure cellular metabolic activity during IH and SH. Cells were seeded at a density of 10,000 cells/well in permeable 96-well plates and cultured at 37°C with conditioned medium of HA. Once at confluence, cells were exposed at IH or SH for 6 h. Control cells under normal atmospheric gas pressure also received the MTT solution. Formazan production was assessed at 570-nm (Multiskan™ RC, Thermo Fisher Scientific, France). Metabolic activity was measured by comparing results from normal atmospheric gas pressure conditions, considered as 100% metabolically active.

Then we also evaluated cell death using a LDH activity method to confirm the least cytotoxic concentrations given by MTT results. Cells were seeded at a density of 10,000 cells/well in permeable 96-well plates and cultured at 37°C with conditioned medium of HA. Once at confluence, cells were exposed at IH or SH for 6 h. Control cells under normal atmospheric gas pressure also used in the LDH test. In this kit, LDH reduces NAD to NADH, which is specifically detected by a colorimetric assay (450-nm).

Imaging plates we use are covered with a sheet of high-performance fluorocarbon film. This film allows very high gas transfer rates. Thus, physiological experiments on cells with exact control of the oxygen partial pressure in the cell microenvironment are possible.

### *Determination of intracellular ROS levels*

To determine ROS activity in our model, we employed The OxiSelect™ Intracellular ROS Assay Kit. Cells were seeded with conditioned medium of HA in permeable 96-well plates and then incubated with dichlorodihydrofluorescein diacetate (DCFH-DA) at 37°C for 1 h. Then cells were exposed to IH or SH for 6 h. After that, fluorescence was read with a fluorimetric plate reader at 480-nm/530-nm. ROS results were determined by comparison with a dichlorodihydrofluorescein (DCF) standard curve.

## *Quantification of HIF-1 $\alpha$ and Nrf2 and during hypoxia and IH*

For both factors, cells were cultured into permeable 96-well plates with conditioned medium of HA for 6 h of IH or SH. Then HIF-1 $\alpha$  and Nrf2 expressions were measured with a cell-based ELISA assay (Cell Biolabs and Aviva Systems Biology) according to the manufacturer's instructions.

## *Barrier properties*

$P_{app}$  was assessed using hydrophilic fluorescent molecules: sodium fluorescein (Na-FI MW = 376 Da) and fluorescein isothiocyanate dextran (FITC-dextran, MW = 4 kDa). Ringer HEPES with 10  $\mu$ g/mL of Na-FI was loaded onto the apical side of the insert and incubated at 37°C for 1 h. Fluorescence was measured with a fluorescence spectrophotometer (Fluoroskan Ascent™, Thermo Fisher Scientific, France) at 485-nm excitation and 530-nm emission wavelengths.  $P_{app}$  is expressed in  $\text{cm}\cdot\text{s}^{-1}$  and was calculated using the formula used in our previous work [Puech, et al. [23]].

TEER was recorded using an EVOM® resistance meter with STX-2 electrodes to characterize the formation of a tight endothelial cell monolayer. One electrode was placed on the luminal side and the other electrode on the abluminal side. The measurement of a blank filter (without cells) was performed and the signal was subtracted from that recorded for the filter with cells. Then the resulting value was reported to the membrane area to obtain the TEER measurement in  $\Omega\cdot\text{cm}^2$ . HBEC-5i with HA conditioned medium reached an optimal steady state plateau at day 14 which was maintained for 5 d. Measurements were then conducted at this time [23].

## *Whole cell ELISA*

Cells were seeded into permeable 96-well permeable plates at a density of 10,000 cells/well and cultured at 37°C with conditioned medium of HA. At confluence, cells were exposed to IH or SH.

Then cells were fixed with 4% paraformaldehyde and permeabilized with methanol with  $\text{H}_2\text{O}_2$ . Claudin-5, ZO-1, VE-cadherin, P-gp and BCRP expressions were evaluated in our model with primary polyclonal antibodies diluted respectively at 2  $\mu$ g/mL, 5  $\mu$ g/mL, 1/200 and 2  $\mu$ g/mL for P-gp and BCRP and incubated at room temperature for 2 h or overnight at 4°C. Secondary IgG antibody diluted 1/2500 or 1/500 was incubated at room temperature for 2 h. Tétraméthylbenzidine (TMB) substrate was added into each well. At the end, the reaction was stopped by addition of 1 N hydrochloric acid and was measured at 450-nm. Our results were normalized with the total protein content as assessed by Coomassie blue total protein assay, according to the manufacturer's instructions.

## *Immunofluorescence assays*

Firstly, cells of inserts were fixed and then permeabilized with glacial methanol (placed at -20°C) for 6 min. The nonspecific sites were then blocked for 30 min at 37°C. The primary antibody was diluted 1/200 in the blocking solution for 1 h at 37°C. The secondary antibody was diluted 1/500 in the blocking solution for 45 min at 37°C. Finally, the nuclei were detected using DAPI diluted 1/1000 in the blocking solution for 30 min at room temperature. The inserts were then placed on glass slides and covered with a Vectashield mounting medium, and glass coverslips were placed on the inserts. The junction staining was performed using an epifluorescence microscope (ZEISS, Axioskop 40) equipped with ZEN software.

## *ABC transporter functional assay by accumulation*

The functionality of two ABC transporters, BCRP and P-gp, was evaluated with accumulation studies. The transport of specific substrates, rhodamine-123 (10  $\mu$ M), with or without inhibitors of BCRP and P-gp was quantified. Cells were cultured with conditioned medium of HA and submitted to normal atmospheric gas pressure, 6 h of IH or SH. Then cells were pretreated with inhibitors: KO-143 (10  $\mu$ M) for BCRP and verapamil (100  $\mu$ M) for P-gp, 15 min at 37°C. Rhodamine-123 was then diluted in each inhibitor solution and incubated for 1 h at 37°C. At the end, cells were washed with cold PBS and lysed with sodium dodecyl sulfate with sodium borate. Fluorescence was measured with a fluorescence spectrophotometer at 485-nm excitation and 530-nm emission wavelengths. Results were expressed as optical density (OD) per mg of total protein.

### Statistical analysis

Data were analyzed using Graphpad Prism 6 software (San Diego, CA, USA). These results are tested by one-way ANOVA (nonparametric) using Tukey's post hoc tests and  $P < 0.05$  was considered as significantly different from controls. Results are presented as sample mean  $\pm$  SEM.

## Results

### Cytotoxicity assays

Before conducting experiments on our model of BBB, we verified that SH and IH did not induce cell death. Cellular toxicity was evaluated with a MTT test and then the LDH activity was measured to evaluate cell death. We chose to perform cycles of IH and SH at 1%  $O_2$  since under normal oxygenation conditions the brain is close to 4.6%  $O_2$  [31]. Indeed, in brain cancers (glioblastoma), considered as highly hypoxic tissue, the oxygenation rate of the tissue is close to 0.7-0.8%  $O_2$  [29]. Actually, there is no standardized protocol for an IH model reflecting the conditions seen in OSA. There are fast cycles [24, 25] and longer cycles [26, 28, 32]. Based on several published papers, we decided to use the following cycles: 35 min hypoxia at 1%  $O_2$  followed by 25 min of reoxygenation at 18%  $O_2$  repeated for 6 cycles. Since no significant cytotoxic effects were observed (Fig. 1), these parameters were chosen for all subsequent experiments.

### Impact of IH on HBEC-5i model

**TEER and  $P_{app}$  measurements.** We could observe the effects of IH and SH on our BBB model composed of endothelial cells cultivated with astrocyte conditioned medium. According to Puech et al. [23], HBEC-5i with HA conditioned medium reached an optimal steady state plateau at day 14 which was maintained for 5 d. The experiments were done when the optimal TEER was obtained. The impact of IH on TEER is shown in Fig. 2A. For IH cycles, TEER decreased significantly by 16.4%, values varied from  $40.8 \pm 0.7$  to  $34.1 \pm 0.5 \Omega \cdot \text{cm}^2$  ( $p < 0.001$ ). Compared to 6 h of SH, we also observed a significant decrease of 19.2% with values from  $40.8 \pm 0.7$  to  $32.9 \pm 0.5 \Omega \cdot \text{cm}^2$  ( $p < 0.001$ ).

$P_{app}$  (Fig. 2B) was measured after 6 h of IH or of SH. For 6h of IH, a significant increase in coefficient permeability of 93.5% was observed with values from  $8 \times 10^{-6} \pm 0.5 \times 10^{-6}$  to  $16.2 \times 10^{-6} \pm 0.08 \times 10^{-5} \text{ cm} \cdot \text{s}^{-1}$  ( $p < 0.001$ ) for Naf-Fl. If we compare this result with 6 h of SH,

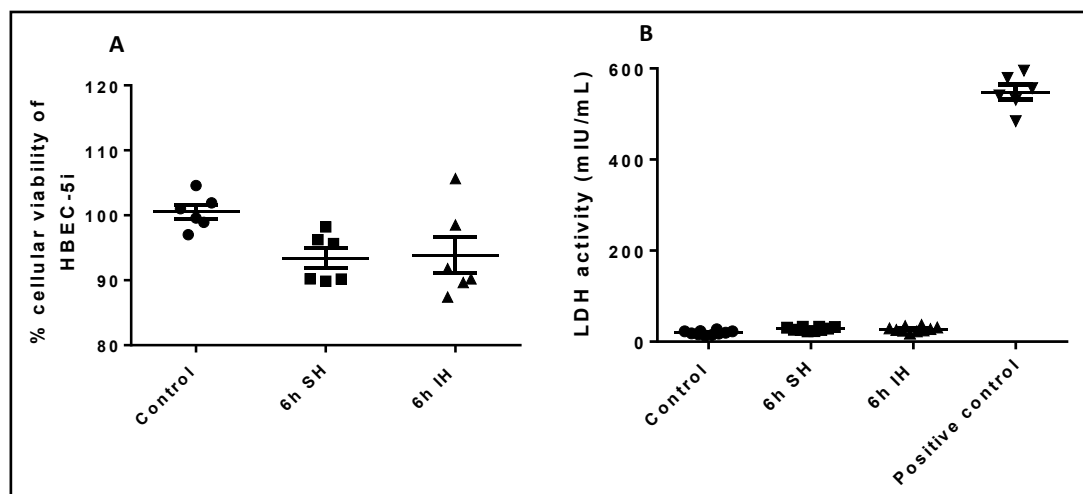


**Fig. 1.** Cytotoxicity effects for 6 h of IH or 6 h of SH in our model of blood-brain barrier measured by a MTT assay (A) and LDH activity method (B). Values are presented as mean value  $\pm$  SEM ( $n=6$ ,  $N=2$  for MTT assay and  $n=10$ ,  $N=2$  for LDH activity). SH: sustained hypoxia, IH: intermittent hypoxia, control: normal atmospheric gas pressure.

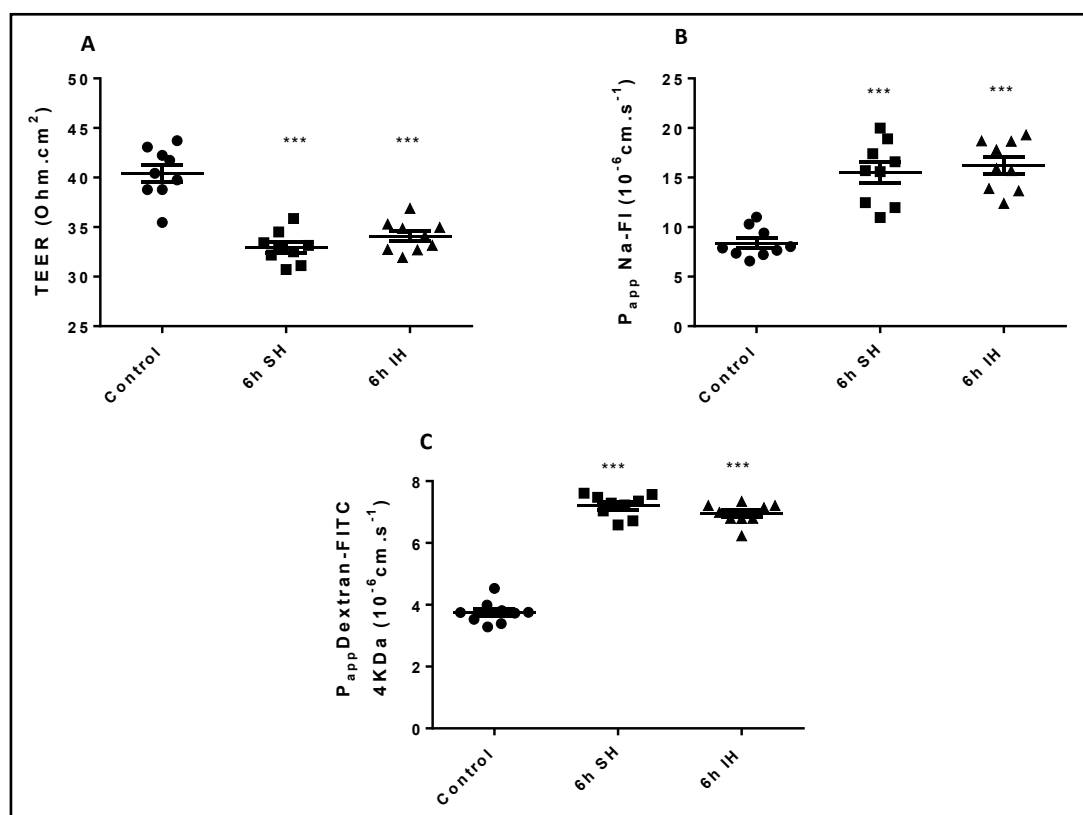


**Fig. 2.** Transendothelial electrical resistance (TEER) (A) and apparent permeability (P<sub>app</sub>) for Na-Fl (B) or FITC-dextran (C) after 6 h of IH or SH in our model of blood-brain barrier. Results are represented as mean value ± SEM (n=9, N=3), \*\*\* p<0.001 compared to control condition. SH: sustained hypoxia, IH: intermittent hypoxia, control: normal atmospheric gas pressure.

we also observed a significant increase of 85% with values between  $8 \times 10^{-6} \pm 0.5 \times 10^{-6}$  to  $15.51 \times 10^{-6} \pm 0.10 \times 10^{-5}$  cm.s<sup>-1</sup> (p<0.001) for Na-Fl. Our results with FITC-dextran confirmed our previous data. We observed a significant increase in coefficient permeability of 89% with values between  $3.8 \times 10^{-6} \pm 1.2 \times 10^{-6}$  to  $7.2 \times 10^{-6} \pm 1.2 \times 10^{-7}$  cm.s<sup>-1</sup> (p<0.001) at 6 h of SH. At 6 h of IH, we also observed a significant increase of 84% with values between  $3.8 \times 10^{-6} \pm 1.2 \times 10^{-6}$  to  $7 \times 10^{-6} \pm 1.13 \times 10^{-7}$  cm.s<sup>-1</sup> (p<0.001).

*Expression of tight (claudin-5, ZO-1) and adherens (VE-cadherin) junctions.* We evaluated how the impact on the tightness of BBB was correlated with an alteration of tight and adherens junctions. VE-cadherin, ZO-1 and claudin-5 are the most represented cell junctions in our model. After 6 h of IH or SH in our *in vitro* BBB model, cell junction expressions were evaluated with whole cell ELISA assay (Fig. 3). For IH, we observed a significant decrease in the expression of all candidate proteins (VE-cadherin, ZO-1 and claudin-5). Expression of VE-cadherin (Fig. 3A) was significantly decreased by 19.7% (p<0.017). For tight junctions, expression of ZO-1 (Fig. 3B) was significantly decreased by 23% (p<0.045) and claudin-5 expression (Fig. 3C) showed a decrease of 27% (p<0.047).

For comparison with 6 h of SH, we observed a higher decrease in expression of each cell junction than IH. Expression of VE-cadherin decreased by 57%, 58% for ZO-1 and 50% for claudin-5 (p<0.001).

In order to illustrate and confirm the results obtained with cell ELISA, we performed immunofluorescence assays on VE-cadherin and ZO-1 junctions. Immunofluorescence VE-cadherin and ZO-1 assays (Fig. 4A and 4B) confirmed whole cells assays; BBB showed important disruptions at cell-cell junction zones at 6 h of IH and 6 h of SH (white arrows, Fig. 4) compared to control.

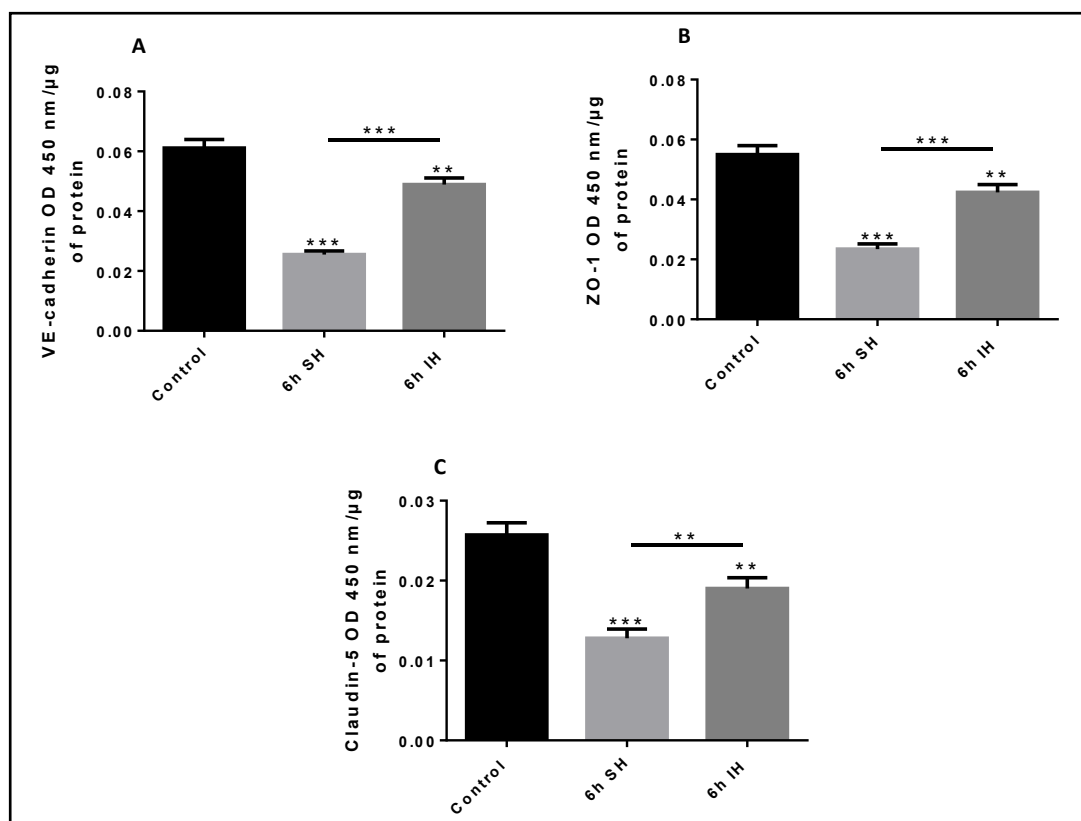


**Fig. 3.** Expressions of VE-cadherin (A), ZO-1 (B) and claudin-5 (C) after exposure of cells to 6 h of IH or SH in our model of blood-brain barrier. Results are represented as mean value  $\pm$  SEM (n=9, N=3), \*\* p $\leq$ 0.01, \*\*\* p $\leq$ 0.001 compared to control conditions. SH: sustained hypoxia, IH: intermittent hypoxia, control: normal atmospheric gas pressure.

#### *Expressions of ABC transporters: BCRP and P-gp*

In several studies, a dysregulation of transporters was observed in response to IH. For this reason, the expression of two main transporters (BCRP and P-gp) were evaluated by whole cell ELISA (Fig. 5). Expression of BCRP (Fig. 5A) significantly decreased by 50% after 6 h of IH (p<0.001). Moreover, after 6 h of SH, a significant decrease of 22% was also observed (p<0.002). In contrast, expression of P-gp (Fig. 5B) showed a significant increase of 68% after 6 h of IH. For 6 h of SH exposure, an even more significant increase of 104% was observed (p<0.001) for this protein.

#### *Functionality of ABC transporters: accumulation studies*

We verified the functionality of ABC transporters in our endothelial cells. For this, rhodamine-123 which is a substrate for both P-gp and BCRP was studied. We looked at the accumulation of rhodamine-123 in endothelial cells with and without inhibitors of BCRP and P-gp (KO143 and verapamil, respectively). Inhibitor concentration and cytotoxicity were measured in previous studies [23]. Inhibitors allowed a better accumulation of Rhodamine 123, proving that these two ABC transporters are functional (Fig. 6). After IH or SH, we observed a global decrease in Rhodamine 123 accumulation, which is more important in SH conditions than IH. This proved that ABC transporters were more active after hypoxia. The use of verapamil allowed an important Rhodamine-123 accumulation in line with a more important expression and functionality of P-gp after hypoxia. Moreover, with KO 143, Rhodamine-123 is more accumulated only after SH conditions, no differences were shown after IH. This discrepancy is in line with a lower BCRP expression after IH reflected the functionality of this protein.

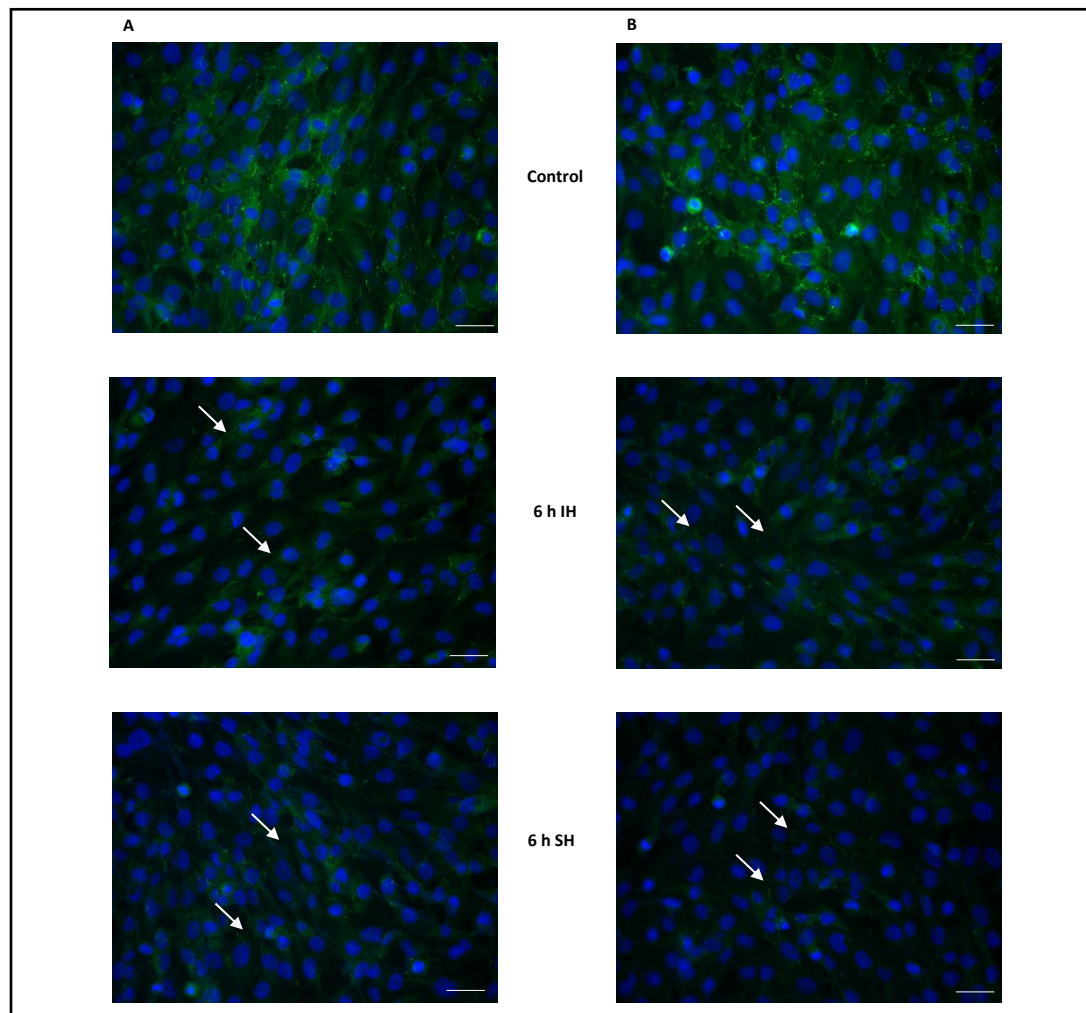


**Fig. 4.** Immunostaining of VE-cadherin (A) or ZO-1 (B) after exposure of cells to 6 h of IH or SH in our model of blood-brain barrier. SH: sustained hypoxia, IH: intermittent hypoxia, control: normal atmospheric gas pressure. Scale bar=100  $\mu$ m.

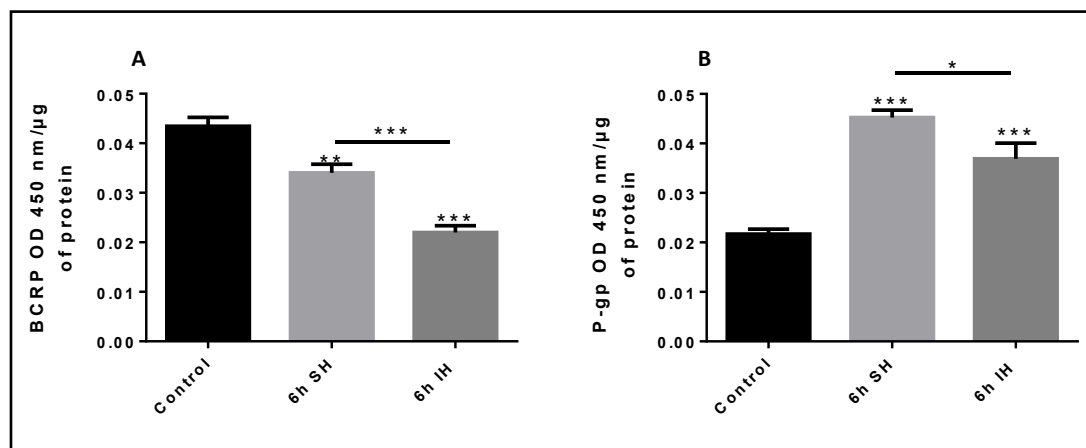
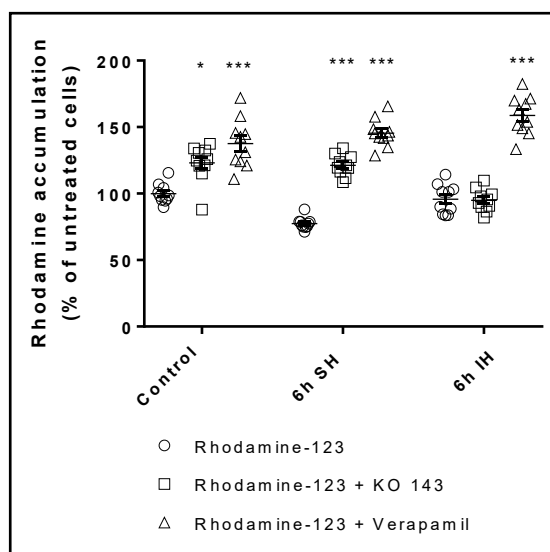


**Fig. 5.** Expressions of BCRP (A) and P-gp (B) after 6 h of IH or SH in our model of blood-brain barrier. Results are represented as mean value  $\pm$  SEM (n = 9, N=3), \*  $p \leq 0.05$ , \*\*  $p \leq 0.01$ , \*\*\*  $p \leq 0.001$  compared to control conditions. SH: sustained hypoxia, IH: intermittent hypoxia, control: normal atmospheric gas pressure, BCRP: breast cancer related protein, P-gp: P-glycoprotein.

**Fig. 6.** Functionality of rhodamine-123 transport by accumulation test with or without specific inhibitors of BCRP (KO 143) and P-gp (verapamil), after exposure of cells to 6 h of SH or IH. Results are represented as mean value  $\pm$  SEM (n=10, N=2), \* $p \leq 0.05$  between rhodamine and rhodamine + KO 143, \*\*\* $p \leq 0.001$  between rhodamine before inhibition versus rhodamine with inhibitors. SH: sustained hypoxia, IH: intermittent hypoxia, control: normal atmospheric gas pressure, BCRP: breast cancer related protein, P-gp: P-glycoprotein.



The measurement of the activity on BCRP was performed despite a significant decrease in its expression in both conditions in order to see if the proteins, although in smaller quantities, would be active or not. In the presence of the competitive BCRP inhibitor, KO143, we observed an increase of 22% in rhodamine-123 accumulation ( $p=0.023$ ). In comparison, in the presence of verapamil, the competitive P-gp inhibitor, we observed an increase of 38% in rhodamine-123 accumulation ( $p<0.001$ ).

First, we showed that after exposure to 6 h of SH, we had a decrease of 23% in rhodamine-123 accumulation ( $p=0.012$ ), showing that ABC activity reflected by a more important efflux was more important after SH. Competitive inhibition with KO143 allowed an increase of 44% in rhodamine-123 accumulation. Competitive inhibition with verapamil allowed a more important increase of 68% ( $p<0.001$ ) in accumulation.

For 6 h of IH, the rhodamine accumulation was the same as observed in control condition. In the presence of KO143, there was a slight but nonsignificant decrease in the accumulation of rhodamine-123, probably related to the underexpression observed in BCRP expression after 6 h of IH. However, with verapamil, we observed a significant increase of 63% in rhodamine-123 accumulation ( $p<0.001$ ), in line with an increase of P-gp expression.

#### *Expressions of ROS, HIF-1 $\alpha$ and Nrf2 in response to IH and SH*

**ROS levels.** As a first step, we verified if IH and SH induced ROS production in our model of BBB with the DCFH-DA assay. The DCFH-DA diffuses through the membrane cell and is then intracellularly converted to hydrophilic DCF. Once in the cells, DCF reacts with ROS allowing its fluorescence to be measured at 570-nm. As shown in Fig. 7, significant increase in fluorescence intensity was detectable after 6 h of SH or IH. For SH, ROS generation showed an important 4-fold increase from  $181.28 \pm 10.9$  to  $722.6 \pm 46.1$  relative fluorescence units (RFU) ( $p<0.001$ ). Under IH conditions, ROS production showed a 3-fold increase from  $181.3 \pm 10.9$  to  $520 \pm 34.3$  RFU ( $p=0.0012$ ).

**HIF-1 $\alpha$  and Nrf2.** IH and SH also regulate several transcription factors such as HIF-1 $\alpha$  and Nrf2. First, we analyzed a key mediator of the cellular response to hypoxia, HIF-1 $\alpha$  (Fig. 8A). IH exposure increased HIF-1 $\alpha$  expression of endothelial cells by 92%. Whereas SH produced a 161% increase in expression of HIF-1 $\alpha$ . Secondly, we analyzed Nrf2 transcription factor, which has an important role in the cellular response to ROS (Fig. 8B). In IH conditions, Nrf2 expression increased by 152%. For SH, an even greater increase was observed with an increase of 200% (all  $p<0.001$ ) in the expression of Nrf2.

**Fig. 7.** ROS production was measured by DCF fluorescence after 6 h of normal atmospheric gas pressure, IH or SH in our model of blood-brain barrier. 1000  $\mu\text{M}$   $\text{H}_2\text{O}_2$  was used as a positive control. DCF fluorescence levels were measured after these conditions. Values are presented as mean value  $\pm$  SEM (n=9, N=3), \*  $p \leq 0.05$ , \*\*  $p \leq 0.01$ , \*\*\*  $p \leq 0.001$  compared to control condition. SH: sustained hypoxia, IH: intermittent hypoxia, control: normal atmospheric gas pressure, ROS: reactive oxygen species, DCF: dichlorodihydrofluorescein.

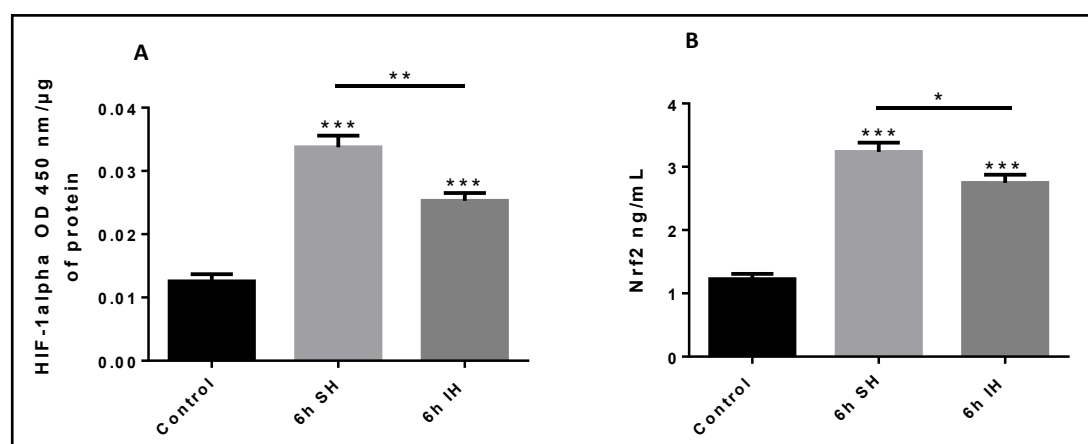
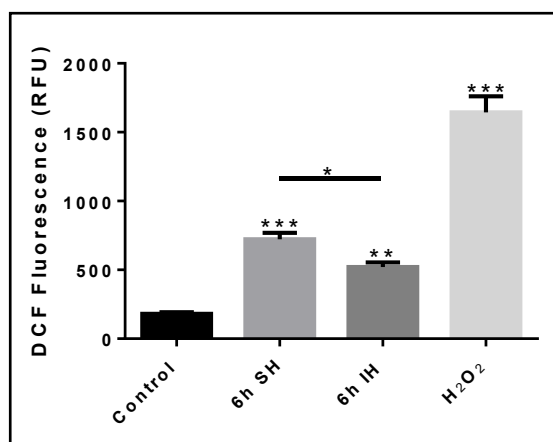


**Fig. 8.** Expressions of HIF-1 $\alpha$  (A), and Nrf2 (B) after exposure of cells 6 h of IH or SH in our model of blood-brain barrier. Results are represented as mean value  $\pm$  SEM (n=9, N=2), \*\*\*  $p \leq 0.001$  compared to control condition. SH: sustained hypoxia, IH: intermittent hypoxia, control: normal atmospheric gas pressure, HIF-1 $\alpha$ : hypoxia-inducible factor 1 alpha, Nrf2: nuclear factor erythroid 2-related factor 2.

## Discussion

OSA is a major health problem characterized by repeated episodes of hypoxia-reoxygenation. IH is associated with high cardiovascular or cerebrovascular risk and cognitive disorders. A hypothesis has emerged the last years that cognitive impairment may be linked to the opening of the BBB and leading to neuronal alteration [4]. In order to better understand the cellular mechanism under IH conditions, an *in vitro* model appeared suitable. We have used the human BBB model developed in our laboratory to study effects of IH.

The BBB, under physiological conditions, protects the brain from blood circulation. Tight and adherent junctions which composed them limit in particular the paracellular passage [33]. Maintaining the homeostasis of the BBB is also possible thanks to the presence of ABC transporters like P-gp or BCRP. In order to better characterize IH effects we have compared these effects with SH effects, which were better established in the literature. Under SH, tight junctions are known to be altered and less expressed at the BBB [34, 35], leading to an increase in paracellular flux. In our study, we could characterized this disruption under SH as expected and published by others [36, 37]. However, few studies have examined the effects of IH on tight and adherens junctions of BBB. After 6 h of IH, we observed an increase in membrane permeability allowing the passage of small molecules such as

Na-Fl or Dextran (Fig. 2). This increased permeability is now known to be associated with a decreased expression of claudin-5, VE-cadherin and ZO-1 (Fig. 3 and 4). After repeated hypoxia-reoxygenation processes, claudin-5 [38] and ZO-1 [39] were altered and showed evidence of an increased permeability of the endothelium of the cerebral microvessels.

We then evaluated the effects of IH on ABC transporters, especially BCRP and P-gp. A decrease in BCRP expression and an increase in P-gp expression were observed for both hypoxic conditions (Fig. 5). Similar data are found in the literature for both SH [22, 40] and IH conditions [41, 42]. Moreover, on ABC transporters there are sites that bind and/or hydrolyze cytoplasmic ATP. Hydrolyzed ATP provides the energy necessary to transport a substrate in one direction against a concentration gradient. To study this effect, we performed functionality tests with a common substrate for BCRP and P-gp using rhodamine-123. Two distinct ways of response were observed and are presented in Fig. 5. Indeed, we observed an increase in activity of P-gp and BCRP in SH correlating with the study of [43]. In contrast, we observed an isolated increase in P-gp activity for IH. This latter result is probably in line with the underexpression of BCRP after 6 h of IH as shown in other study [44]. This decrease was not linked to ATP level because we had observed an increase in activity of P-gp at the same time, and we did not observe the same effects between SH and IH. Moreover, there is strong cooperation between P-gp and BCRP. It is recognized that in the absence of activity of one of them, the other membrane protein is sufficient to prevent the entry of compounds into the brain [45].

In response to hypoxia, many mechanisms are activated like stress oxidative and hypoxia pathway. In our work, we evaluated two transcription factors Nrf2 and HIF-1 $\alpha$ . Initially, oxidative stress is observed, leading to the production of ROS [46–48]. Regulation of ROS is essential for maintaining cellular homeostasis. In response to the production of ROS, the transcription factor Nrf2 increases and gives the cell the ability to produce antioxidant factors which reduce the damaging impact of intracellular ROS [20]. We demonstrated that IH like SH could also induce transcription factors sensitive to the oxygen content of endothelial cells, hypoxia inducible factors and in particular HIF-1 $\alpha$ . Furthermore, Nrf2 and HIF-1 $\alpha$  signalling are both regulated by the presence of ROS [49]. These two conditions allowed a significant increase in ROS (Fig. 7). Our results are in agreement with the literature: an increase in ROS in acute hypoxic conditions in the endothelial cells of BBB [50] or in other tissues such as nasal polyp-derived fibroblasts [51]. The same observation is found in conditions of IH in the BBB [52–54]. Furthermore, this increase in ROS is directly correlated with an increase in HIF-1 $\alpha$  and/or Nrf2 activity (Fig. 8). Indeed, the expression of HIF-1 $\alpha$  known to increase under hypoxic conditions is correlated with ROS production [32]. Thus, in line with the literature we observed a higher expression of this factor in SH compared to IH conditions [55]. The production of ROS under SH or IH conditions is also known in the literature to increase the expression of Nrf2 [56], which is essential for regulating responses to oxidative stress. Moreover, the longer the duration of hypoxia, the greater is the expression of Nrf2 [57].

In our study, the expression of junction proteins is much lower under SH conditions, which can be explained by the higher ROS production in our model. Indeed, the production of ROS is known to alter BBB functioning. Schreiber et al. [58] showed that ROS activate a cascade leading to a rearrangement of the cytoskeleton and the disappearance of tight junctions including claudin-5 in the BBB. Moreover, disorganization/breakdown of these junctions is associated with excessive production of ROS found in many neurodegenerative disorders like Alzheimer's or Parkinson's diseases [59]. In addition, HIF-1 $\alpha$  also a candidate to BBB alteration is more expressed in SH than in IH, which may explain the expression of more altered junction proteins in SH [36]. In addition, a downstream gene of HIF-1 $\alpha$  that would be very interesting to look at is the vascular endothelial growth factor (VEGF). Indeed, this factor increases in hypoxic conditions through the HIF-1 $\alpha$  pathway and leads notably to an increase in permeability of the BBB, associated with an alteration of the junctions [37]. Conversely, Nrf2 is significantly increased in both conditions and allows protection of the

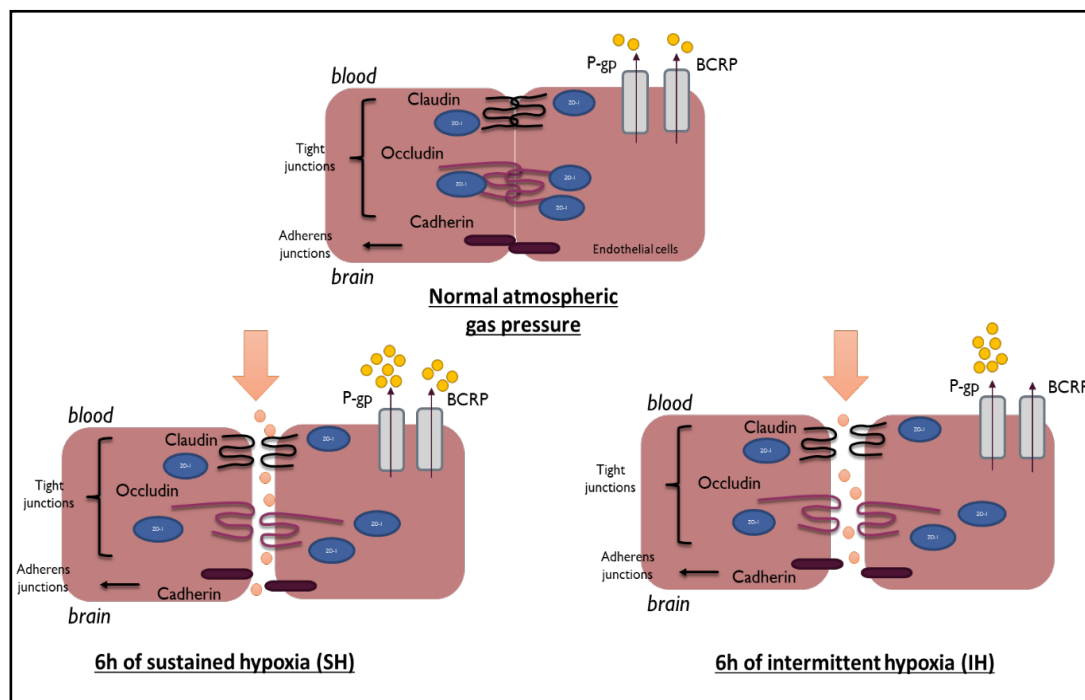


**Fig. 9.** Representation of the tight, adherens junctions within the endothelial cells in our model of blood-brain barrier. Tightly joined and functional endothelial cells under normal atmospheric gas pressure. Opening of the paracellular pathway under SH and IH, and alteration in P-gp - BCRP expression/activity. BCRP: breast cancer related protein, P-gp: P-glycoprotein.

BBB tight junctions and explain protein expression observed under IH. IH as well as SH are deleterious for the organization and the functionality of brain microvascular endothelial cells (Fig. 9).

Regarding ABC transporters, under both hypoxic conditions there is an increase in the expression and functionality of P-gp. Nrf2 and HIF-1 $\alpha$  are known to upregulate this protein in different biostress conditions such as tumorigenesis or post epileptic stress [21, 60, 61]. By contrast, Nrf2 positively regulates BCRP under hypoxia [62]. In our model, expressions of BCRP are reduced in both hypoxic conditions, but the decrease is more severe under IH. The activity of BCRP is preserved under SH but not in IH, suggesting that other adaptative mechanisms associated with SH are involved. Indeed, a downregulation of BCRP expression is also observed under inflammatory conditions, particularly when placentas are exposed to viral or bacterial infection [63]. Acute low-grade systemic inflammation is present in patients with OSA and may contribute to BCRP suppression at the protein level in the BBB [42]. In addition, a recent study published by our laboratory on the effects of serum from patients with sleep apnea showed a downregulation of the expression and functionality of BCRP in our BBB model [44] (Fig. 10).

According to various studies, HIF-1 $\alpha$  and Nrf2 are closely involved in the mutual promotion and stabilization of their expression during hypoxia [64]. A recent study demonstrated a link between Nrf2 and HIF-1 $\alpha$ . The activation of the Nrf2 factor would be responsible for both the expression of HIF1 $\alpha$  and its stabilization. In addition, two genes produced by Nrf2 would also be able to increase its stability [49]. In another study, it is the expression of the HIF-1 $\alpha$  gene that is involved in the promotion of Nrf2 [57]. Therefore, the coordinated increase in the expression of Nrf2 and HIF1 $\alpha$  triggered notably by the production of ROS in IH and SH showed a crosstalk between these two factors in our study.

The methodological limitations of our study are essentially linked to the relative slowness of adaptation of the system regulating hypoxia for the conditions of IH. These

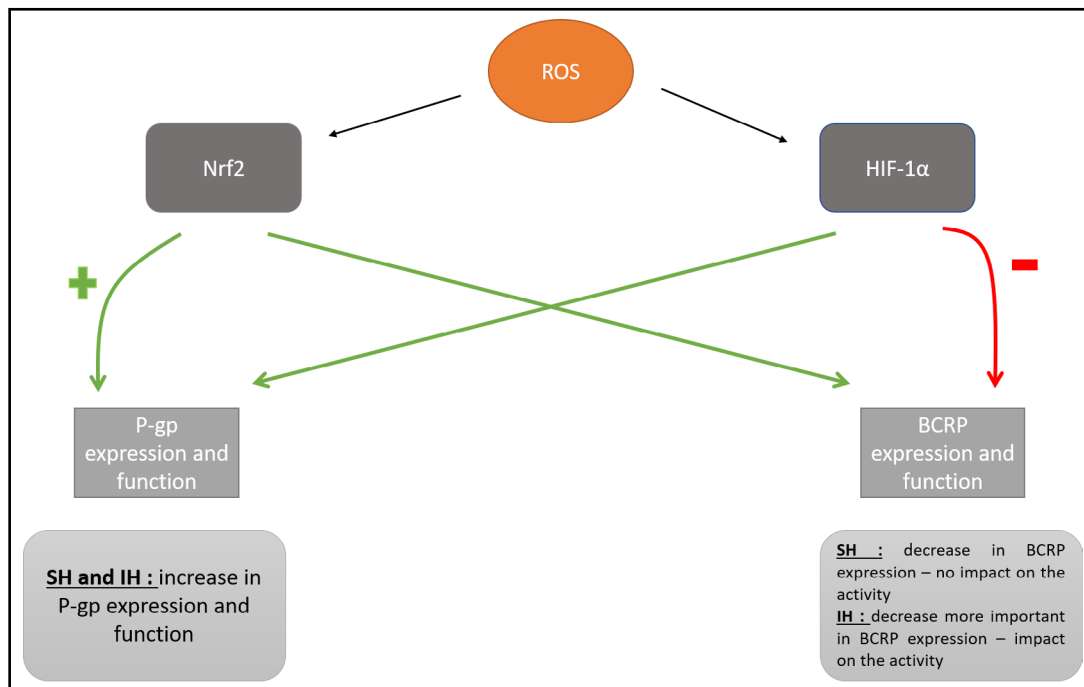


**Fig. 10.** One hypothesis of regulation of BCRP and P-gp transporters by HIF-1 $\alpha$  and Nrf2 under IH and SH. ROS: reactive oxygen species, HIF-1 $\alpha$ : hypoxia-inducible factor 1 alpha, Nrf2: nuclear factor erythroid 2-related factor 2, BCRP: breast cancer related protein, P-gp: P-glycoprotein, IH: intermittent hypoxia, SH: sustained hypoxia.

transitions are slower than in OSA clinical situations. In addition, the cyclicity of the phenomena of desaturation and reoxygenation are much longer with our device than in the clinical situation of obstructive apnea. Indeed, our cycles duration is long, but this represent a first interesting approach of the delayed effect between sustained hypoxia and intermittent hypoxia. In humans as in animal models it is very difficult to know precisely the partial pressure of oxygen present during apneic phenomena in the cerebral microvascular blood compartment. Estimates are made from brain tissue PO<sub>2</sub> measurements which are not very precise. However, our results on BBB cellular models are consistent with brain imaging data obtained in apneic patients. These very reproducible results confirm in our opinion in IH as well in SH an opening of the BBB (at least one functional alteration) involving the protein tight junctions as well as the ABC transporters.

## Conclusion

Our model of IH tested on an *in vitro* model of the human BBB is innovative for understanding the underlying mechanisms affecting the brain in the pathology of sleep apnea. IH generated by our repeated cycles induced the expression of various factors during hypoxic stress, including expression modulations of Nrf2 which has been little explored under IH conditions. The consequences of the stress are an opening of the paracellular pathway and a dysregulated activity of the ABC transporters. Finally, these results also highlight that the mechanisms involved in response to IH differ from those under SH and are important in order to propose new strategies to limit the potential cerebral consequences of respiratory related sleep disorders.

## Acknowledgements

### *Author Contributions*

Cindy Zolotoff: Conceptualization, Methodology, Investigations, Formal analysis, Writing - Original Draft; Anne-Cloé Voirin: Methodology, Formal analysis; Clémentine Puech: Methodology, Formal analysis; Frédéric Roche and Nathalie Perek: Conceptualization, Validation, Supervision, Writing - Review & Editing.

### *Statement of Ethics*

The authors have no ethical conflicts to disclose.

## Disclosure Statement

The authors have no conflicts of interest to declare.

## References

- 1 Guilleminault C, Tilkian A, Dement WC: The sleep apnea syndromes. *Annu Rev Med* 1976;27:465–484.
- 2 Semenza GL: Hypoxia-Inducible Factor 1 and Cardiovascular Disease. *Annu Rev Physiol* 2014;76:39–56.
- 3 Iyalomhe O, Swierczek S, Enwerem N, Chen Y, Adedeji MO, Allard J, Ntekim O, Johnson S, Hughes K, Kurian P, Obisesan TO: The Role of Hypoxia-Inducible Factor 1 in Mild Cognitive Impairment. *Cell Mol Neurobiol* 2017;37:969–77.
- 4 Lim DC, Pack AI: Obstructive sleep apnea and cognitive impairment: Addressing the blood–brain barrier. *Sleep Med Rev* 2014;18:35–48.
- 5 Dyrna F, Hanske S, Krueger M, Bechmann I: The Blood-Brain Barrier. *J Neuroimmune Pharmacol* 2013;8:763–773.
- 6 Wolburg H, Noell S, Mack A, Wolburg-Buchholz K, Fallier-Becker P: Brain endothelial cells and the gliovascular complex. *Cell Tissue Res* 2009;335:75–96.
- 7 Wolburg H, Lippoldt A: Tight junctions of the blood–brain barrier: development, composition and regulation. *Vascu Pharmacol* 2002;38:323–337.
- 8 Anderson JM, Van Itallie CM: Tight junctions and the molecular basis for regulation of paracellular permeability. *Am J Physiol* 1995;269:G467–G475.
- 9 Löscher W, Potschka H: Blood-Brain Barrier Active Efflux Transporters: ATP-Binding Cassette Gene Family. *NeuroRx* 2005;2:86–98.
- 10 Komori H, Yamada K, Tamai I: Hyperuricemia enhances intracellular urate accumulation via down-regulation of cell-surface BCRP/ABCG2 expression in vascular endothelial cells. *Biochim Biophys Acta Biomembr* 2018;1860:973–980.
- 11 Kondoh M, Ohga N, Akiyama K, Hida Y, Maishi N, Towfik AM, Inoue N, Shindoh M, Hida K: Hypoxia-Induced Reactive Oxygen Species Cause Chromosomal Abnormalities in Endothelial Cells in the Tumor Microenvironment. *PLOS One* 2013;8:e80349.
- 12 Debevec T, Millet GP, Pialoux V: Hypoxia-Induced Oxidative Stress Modulation with Physical Activity. *Front Physiol* 2017 Feb 13;8:84.
- 13 Tafani M, Sansone L, Limana F, Arcangeli T, De Santis E, Polese M, Fini M, Russo MA: The Interplay of Reactive Oxygen Species, Hypoxia, Inflammation, and Sirtuins in Cancer Initiation and Progression. *Oxid Med Cell Longev* 2016;2016:3907147.
- 14 Mittal M, Siddiqui MR, Tran K, Reddy SP, Malik AB: Reactive Oxygen Species in Inflammation and Tissue Injury. *Antioxid Redox Signal* 2014;20:1126–1167.
- 15 Pun PBL, Lu J, Mochhala S: Involvement of ROS in BBB dysfunction. *Free Radic Res* 2009;43:348–364.
- 16 Guzy RD, Hoyos B, Robin E, Chen H, Liu L, Mansfield KD, Simon MC, Hammerling U, Schumacker PT: Mitochondrial complex III is required for hypoxia-induced ROS production and cellular oxygen sensing. *Cell Metab* 2005;1:401–408.

- 17 Carmeliet P, Dor Y, Herbert JM, Fukumura D, Brusselmans K, Dewerchin M, Neeman M, Bono F, Abramovitch R, Maxwell P, Koch CJ, Ratcliffe P, Moons L, Jain RK, Collen D, Keshert E, Keshet E: Role of HIF-1alpha in hypoxia-mediated apoptosis, cell proliferation and tumour angiogenesis. *Nature* 1998;394:485–490.
- 18 Liu W, Shen SM, Zhao XY, Chen GQ: Targeted genes and interacting proteins of hypoxia inducible factor-1. *Int J Biochem Mol Biol* 2012;3:165–178.
- 19 Itoh K, Chiba T, Takahashi S, Ishii T, Igarashi K, Katoh Y, Oyake T, Hayashi N, Satoh K, Hatayama I, Yamamoto M, Nabeshima Y: An Nrf2/small Maf heterodimer mediates the induction of phase II detoxifying enzyme genes through antioxidant response elements. *Biochem Biophys Res Commun* 1997;236:313–322.
- 20 Kaspar JW, Niture SK, Jaiswal AK: Nrf2:INrf2 (Keap1) signaling in oxidative stress. *Free Radic Biol Med* 2009;47:1304–1309.
- 21 Ding Z, Yang L, Xie X, Xie F, Pan F, Li J, He J, Liang H: Expression and significance of hypoxia-inducible factor-1 alpha and MDR1/P-glycoprotein in human colon carcinoma tissue and cells. *J Cancer Res Clin Oncol* 2010;136:1697–1707.
- 22 Francois LN, Gorczyca L, Du J, Bircsak KM, Yen E, Wen X, Tu MJ, Yu A, Illsley NP, Zamudio S, Aleksunes LM: Down-regulation of the placental BCRP/ABCG2 transporter in response to hypoxia signaling. *Placenta* 2017;51:57–63.
- 23 Puech C, Hodin S, Forest V, He Z, Mismetti P, Delavenne X, Perek N: Assessment of HBEC-5i endothelial cell line cultivated in astrocyte conditioned medium as a human blood-brain barrier model for ABC drug transport studies. *Int J Pharm* 2018;551:281–289.
- 24 Kumar GK, Kim DK, Lee MS, Ramachandran R, Prabhakar NR: Activation of tyrosine hydroxylase by intermittent hypoxia: involvement of serine phosphorylation. *J Appl Physiol* (1985) 2003;95:536–544.
- 25 Yuan G, Adhikary G, McCormick AA, Holcroft JJ, Kumar GK, Prabhakar NR: Role of oxidative stress in intermittent hypoxia-induced immediate early gene activation in rat PC12 cells. *J Physiol* 2004;557:773–783.
- 26 Dyugovskaya L, Polyakov A, Lavie P, Lavie L: Delayed neutrophil apoptosis in patients with sleep apnea. *Am J Respir Crit Care Med* 2008;177:544–554.
- 27 Gozal E, Sachleben LR, Rane MJ, Vega C, Gozal D: Mild sustained and intermittent hypoxia induce apoptosis in PC-12 cells via different mechanisms. *Am J Physiol Cell Physiol* 2005;288:C535–C542.
- 28 Toffoli S, Feron O, Raes M, Michiels C: Intermittent hypoxia changes HIF-1alpha phosphorylation pattern in endothelial cells: unravelling of a new PKA-dependent regulation of HIF-1alpha. *Biochim Biophys Acta* 2007;1773:1558–1571.
- 29 Hunyor I, Cook KM: Models of intermittent hypoxia and obstructive sleep apnea: molecular pathways and their contribution to cancer. *Am J Physiol Regul Integr Comp Physiol* 2018;315:R669–R687.
- 30 Abbott NJ: Astrocyte-endothelial interactions and blood-brain barrier permeability. *J Anat* 2002;200:629–638.
- 31 Carreau A, El Hafny-Rahbi B, Matejuk A, Grillon C, Kieda C: Why is the partial oxygen pressure of human tissues a crucial parameter? Small molecules and hypoxia. *J Cell Mol Med* 2011;15:1239–1253.
- 32 Martinive P, Defresne F, Quaghebeur E, Daneau G, Crokart N, Grégoire V, Gallez B, Dessy C, Feron O: Impact of cyclic hypoxia on HIF-1α regulation in endothelial cells – new insights for anti-tumor treatments. *FEBS J* 2009;276:509–518.
- 33 Daneman R, Prat A: The Blood-Brain Barrier. *Cold Spring Harb Perspect Biol* 2015;7:a020412.
- 34 Fischer S, Wobben M, Marti HH, Renz D, Schaper W: Hypoxia-Induced Hyperpermeability in Brain Microvessel Endothelial Cells Involves VEGF-Mediated Changes in the Expression of Zonula Occludens-1. *Microvasc Res* 2002;63:70–80.
- 35 Wu LW, Yin F, Peng J, Wang W-D, Gan N: The tight junction proteins ZO-1, occludin and actin participate in the permeability increasing of blood-brain barrier induced by hypoxia-ischemia. *Zhongguo Dang Dai Er Ke Za Zhi* 2008;10:513–516.
- 36 Engelhardt S, Al-Ahmad AJ, Gassmann M, Ogunshola OO: Hypoxia selectively disrupts brain microvascular endothelial tight junction complexes through a hypoxia-inducible factor-1 (HIF-1) dependent mechanism. *J Cell Physiol* 2014;229:1096–1105.
- 37 Yeh WL, Lu DY, Lin CJ, Liou HC, Fu WM: Inhibition of Hypoxia-Induced Increase of Blood-Brain Barrier Permeability by YC-1 through the Antagonism of HIF-1α Accumulation and VEGF Expression. *Mol Pharmacol* 2007;72:440–449.

- 38 Zhao H, Zhang Q, Xue Y, Chen X, Haun RS: Effects of hyperbaric oxygen on the expression of claudins after cerebral ischemia–reperfusion in rats. *Exp Brain Res* 2011;212:109–117.
- 39 Jiao H, Wang Z, Liu Y, Wang P, Xue Y: Specific Role of Tight Junction Proteins Claudin-5, Occludin, and ZO-1 of the Blood–Brain Barrier in a Focal Cerebral Ischemic Insult. *J Mol Neurosci* 2011;44:130–139.
- 40 Chatard M, Puech C, Roche F, Perek N: Hypoxic Stress Induced by Hydralazine Leads to a Loss of Blood-Brain Barrier Integrity and an Increase in Efflux Transporter Activity. *PLoS One* 2016;11:e0158010.
- 41 Dopp JM, Moran JJ, Abel NJ, Wiegert NA, Cowgill JB, Olson EB, Sims JJ: Influence of intermittent hypoxia on myocardial and hepatic P-glycoprotein expression in a rodent model. *Pharmacotherapy* 2009;29:365–372.
- 42 Poller B, Drewe J, Krähenbühl S, Huwyler J, Gutmann H: Regulation of BCRP (ABCG2) and P-glycoprotein (ABCB1) by cytokines in a model of the human blood-brain barrier. *Cell Mol Neurobiol* 2010;30:63–70.
- 43 Krishnamurthy P, Schuetz JD: The ABC Transporter Abcg2/Bcrp: Role in Hypoxia Mediated Survival. *Biometals* 2005;18:349–358.
- 44 Voirin AC, Celle S, Perek N, Roche F: Sera of elderly obstructive sleep apnea patients alter blood–brain barrier integrity in vitro: a pilot study. *Scientific Reports* 2020;10:11309.
- 45 Agarwal S, Hartz AMS, Elmquist WF, Bauer B: Breast Cancer Resistance Protein and P-glycoprotein in Brain Cancer: Two Gatekeepers Team Up. *Curr Pharm Des* 2011;17:2793–2802.
- 46 Lavie L: Obstructive sleep apnoea syndrome--an oxidative stress disorder. *Sleep Med Rev* 2003;7:35–51.
- 47 Li L, Ren F, Qi C, Xu L, Fang Y, Liang M, Feng J, Chen B, Ning W, Cao J: Intermittent hypoxia promotes melanoma lung metastasis via oxidative stress and inflammation responses in a mouse model of obstructive sleep apnea. *Respiratory Research* 2018;19:28.
- 48 Wang Y, Zhang SXL, Gozal D: Reactive oxygen species and the brain in sleep apnea. *Respir Physiol Neurobiol* 2010;174:307–316.
- 49 Lacher SE, Levings DC, Freeman S, Slattery M: Identification of a functional antioxidant response element at the HIF1A locus. *Redox Biol* 2018;19:401–411.
- 50 Al Ahmad A, Gassmann M, Ogunshola OO: Involvement of oxidative stress in hypoxia-induced blood–brain barrier breakdown. *Microvascular Research* 2012;84:222–225.
- 51 Moon YM, Kang HJ, Cho JS, Park IH, Lee HM: Nox4 mediates hypoxia-stimulated myofibroblast differentiation in nasal polyp-derived fibroblasts. *Int Arch Allergy Immunol* 2012;159:399–409.
- 52 Lochhead JJ, McCaffrey G, Quigley CE, Finch J, DeMarco KM, Nametz N, Davis TP: Oxidative stress increases blood-brain barrier permeability and induces alterations in occludin during hypoxia-reoxygenation. *J Cereb Blood Flow Metab* 2010;30:1625–1636.
- 53 Won S, Sayeed I, Peterson BL, Wali B, Kahn JS, Stein DG: Vitamin D Prevents Hypoxia/Reoxygenation-Induced Blood-Brain Barrier Disruption via Vitamin D Receptor-Mediated NF-kB Signaling Pathways. *PLoS One* 2015;10:e0122821.
- 54 Zehendner CM, Librizzi L, Hedrich J, Bauer NM, Angamo EA, de Curtis M, Luhmann HJ: Moderate Hypoxia Followed by Reoxygenation Results in Blood-Brain Barrier Breakdown via Oxidative Stress-Dependent Tight-Junction Protein Disruption. *PLoS One* 2013;8:e82823.
- 55 Ryan Silke, Taylor Cormac T., McNicholas Walter T: Selective Activation of Inflammatory Pathways by Intermittent Hypoxia in Obstructive Sleep Apnea Syndrome. *Circulation* 2005;112:2660–2667.
- 56 Kolamunne RT, Dias IH, Vernallis AB, Grant MM, Griffiths HR: Nrf2 activation supports cell survival during hypoxia and hypoxia/reoxygenation in cardiomyoblasts; the roles of reactive oxygen and nitrogen species. *Redox Biol* 2013;1:418–426.
- 57 Ji W, Wang L, He S, Yan L, Li T, Wang J, Kong ANT, Yu S, Zhang Y: Effects of acute hypoxia exposure with different durations on activation of Nrf2-ARE pathway in mouse skeletal muscle. *PLoS One* 2018;13:e0208474.
- 58 Schreibelt G, Kooij G, Reijkerkerk A, van Doorn R, Gringhuis SI, van der Pol S, Weksler BB, Romero IA, Couraud PO, Piontek J, Blasig IE, Dijkstra CD, Ronken E, de Vries HE: Reactive oxygen species alter brain endothelial tight junction dynamics via RhoA, PI3 kinase, and PKB signaling. *FASEB J* 2007;21:3666–3676.
- 59 Maiuolo J, Gliozzi M, Musolino V, Scicchitano M, Carresi C, Scarano F, Bosco F, Nucera S, Ruga S, Zito MC, Mollace R, Palma E, Fini M, Muscoli C, Mollace V: The “Frail” Brain Blood Barrier in Neurodegenerative Diseases: Role of Early Disruption of Endothelial Cell-to-Cell Connections. *Int J Mol Sci* 2018;19:2693.
- 60 Jeddi F, Soozangar N, Sadeghi MR, Somi MH, Shirmohamadi M, Eftekhari-Sadat AT, Samadi N: Nrf2 overexpression is associated with P-glycoprotein upregulation in gastric cancer. *Biomed Pharmacother* 2018;97:286–292.

- 61 Merelli A, Ramos AJ, Lazarowski A, Auzmendi J: Convulsive Stress Mimics Brain Hypoxia and Promotes the P-Glycoprotein (P-gp) and Erythropoietin Receptor Overexpression. Recombinant Human Erythropoietin Effect on P-gp Activity. *Front Neurosci* 2019;13:750.
- 62 Ibbotson K, Yell J, Ronaldson PT: Nrf2 signaling increases expression of ATP-binding cassette subfamily C mRNA transcripts at the blood-brain barrier following hypoxia-reoxygenation stress. *Fluids Barriers CNS* 2017;14:6.
- 63 Lye P, Bloise E, Nadeem L, Peng C, Gibb W, Ortiga-Carvalho TM, Lye SJ, Matthews SG: Breast Cancer Resistance Protein (BCRP/ABCG2) Inhibits Extra Villous Trophoblast Migration: The Impact of Bacterial and Viral Infection. *Cells* 2019;8:1150.
- 64 Toth RK, Warfel NA: Strange Bedfellows: Nuclear Factor, Erythroid 2-Like 2 (Nrf2) and Hypoxia-Inducible Factor 1 (HIF-1) in Tumor Hypoxia. *Antioxidants (Basel)* 2017;6:27.